

Beam Tracking for UAV-Assisted FSO Links With a Four-Quadrant Detector

Hossein Safi, Akbar Dargahi, and Julian Cheng, *Senior Member, IEEE*

Abstract

A ground-to-air free-space optical link is studied for a hovering unmanned aerial vehicle (UAV) having multiple rotors. For this UAV, a four-quadrant array of photodetectors is used at the optical receiver to alleviate the adverse effect of hovering fluctuations by enlarging the receiver field-of-view. Extensive mathematical analysis is conducted to evaluate the beam tracking performance under the random effects of hovering fluctuations. The accuracy of the derived analytical expressions is corroborated by performing Monte-Carlo simulations. It is shown that the performance of such links depends heavily on the random fluctuations of hovering UAV, and, for each level of instability there is an optimal size for the array that minimizes the tracking error probability

Index Terms

FSO, four-quadrant detector, UAV.

I. INTRODUCTION

Recently, unmanned aerial vehicle (UAV) communications have attracted significant interest due to many advantageous such as fast deployment, flexible configuration, and possibility of having better channel conditions. Furthermore, technological advances of UAVs along with their reduced production costs have made future cellular networks more likely to be equipped with UAVs as flying base stations (BSs) [1]. Nevertheless, existing terrestrial wireless networks may experience radio interference when UAVs are used as aerial BSs, making it challenging to implement a practical aerial RF link. UAVs and free-space optical (FSO) based communication systems have been recently proposed as a promising approach for the next generation wireless network [2], where the aerial communication links are free of radio interference. FSO links offer higher bandwidth and security than the conventional RF

H. Safi and A. Dargahi are with the Department of Electrical Engineering, Shahid Beheshti University G. C., 1983963113, Tehran, Iran (e-mail: {h_safi, adargahi}@sbu.ac.ir). J. Cheng is with the School of Engineering, The University of British Columbia, V1V 1V7, Kelowna, BC, Canada (email:julian.cheng@ubc.ac)

links, and thus, they can play a pivotal role in supporting emerging data-hungry applications. It is of great importance for the optical transmitter in a UAV-assisted FSO link to point precisely at the receiver field-of-view (FoV) in order to avoid beam misalignment. However, when optical subsystems are mounted on a hovering UAV, orientation deviations (due to the UAV's random wobbling) can cause angle of arrival (AoA) fluctuations of optical beam at the lens aperture, and, subsequently, image beam will dance around the area of photodetector (PD) [3]. Hence, for an optical link from a ground node towards a UAV-based receiver, it becomes unavoidable to perform beam tracking to determine the direction of arrival beam at the receiver plane and re-establish the link in the case of beam misalignment.

For terrestrial FSO links where transceivers are firmly fixed, the effect of AoA fluctuations can be neglected. Indeed, most of the literature in the context of optical beam tracking has been dedicated to space optics, i.e., inter-satellite links and earth-space laser communication [4]. Moreover, an extensive survey was conducted on different acquisition, tracking, and pointing (ATP) methods for mobile FSO communications, and different use cases of those methods were categorized [5]. However, most of the existing methods require heavy and bulky mechanical or piezoelectric equipment, e.g., gimbals and retro reflectors, which are inappropriate for small-sized multi-rotor UAVs with limited payload.

To relax practical constraints imposed by payload and power consumption limitations while combating the adverse effects of AoA fluctuations, a practical and cost-effective solution is to replace the ATP unit on the small UAV with an array of PDs [4], [6], which gives three practical advantages. First, the receiver FoV can be made wider to compensate the adverse effect of AoA fluctuations on the system performance. Second, the sophisticated ATP subsystem is moved to the optical transceiver on the ground station. Third, the instantaneous orientation errors can be fixed by estimating the position of the beam on the array (i.e., the AoA of the beam), and feeding it back through a control message to the mechanical subsystem of the UAV¹.

Optical beam tracking using detector arrays has recently been studied assuming the photon-counting regime, e.g., a deep-space optical communication setting [7]–[10]. For instance, the photodetection was modeled by a non-homogeneous Poisson process [7], and two filtering methods, i.e., a Kalman filter and a particle filter, were proposed for tracking the beam position. In addition, a mathematical analysis was performed to show that the probability of

¹Here, we assume that the UAV orients itself or use a simple servo motor (which has much lower weight and price than a bulky stabilizer) to align detector plane towards the ground transmitter.

error decreases monotonically as the number of PD in the array is increased [8]. Meanwhile, the beam position estimation problem was examined [9] for photon-counting detector arrays and the Cramér-Rao lower bounds were derived for the variance of unbiased estimators. Furthermore, beam tracking algorithms were proposed [10] using received photon counts during an observation interval as a sufficient statistic for tracking the beam position.

Nevertheless, the results of these prior works are applicable to photon-limited channels of deep space or long-range FSO communications in which the long link distances reduce the number of received signal photons significantly. Although such systems can deliver a better performance than conventional ones with direct detection, but at the expense of higher implementation cost. In addition, if a UAV-based FSO system is considered as an aerial access point in the backhaul or fronthaul link of next generation wireless networks, the received optical power must be high enough to accommodate the high quality-of-service demand of such systems, e.g., bit-error rate (BER) lower than 10^{-9} . In such a high received power regime, the output of the photodetectors is well approximated by a Gaussian distribution [11].

The main contribution of this letter is the mathematical analysis carried out to derive the tracking error probability when a four-quadrant array of PDs is used at the optical receiver. In particular, this analysis assumes a Gaussian distribution of the output of the PDs, and incorporates the combined effects of atmospheric turbulence, pointing error induced geometrical loss, the size of the PDs in the array, and AoA fluctuations of the received optical beam. We provide simulation results to verify the accuracy of the derived analytical expressions and study the effect of hovering fluctuations on the system performance. Indeed, simulation results show that the performance of such links depends heavily on the random fluctuations of the hovering UAV. Also, it is shown that enlarging the receiver field-of-view via employing the array of detectors can help alleviate the adverse effects of random hovering fluctuations on the link performance. Furthermore, the results show that for each level of instability there is an optimal size for the array that minimizes the tracking error probability. Since estimating the beam position at the receiver is part of the channel information required for data detection, minimizing tracking error will ultimately improve system performance in terms of BER.

To the best of authors' knowledge, there is little work in the literature that mathematically models beam tracking error under random orientation fluctuations by taking into account the effects of all channel impairments in an intensity modulation direct detection (IM/DD) FSO system.

II. SYSTEM MODEL

A. Signal Model

We consider an IM/DD FSO system with on-off keying signaling. The received signal at the i th quadrant corresponding to the k th symbol interval is given as

$$r_i[k] = hD_i s[k] + n_i[k], \quad \text{for } i \in \{1, \dots, 4\} \quad (1)$$

where $s[k]$ denotes the transmitted symbol with optical power P_t , and h denotes the fading channel coefficient, which is assumed to be constant over a large sequence number of transmitted bits (i.e., quasi static property). Let us define $D_i \in \{0, 1\}$ as a signal indicator, i.e., $D_i = 1$ indicates that the received beam is captured by the i th quadrant. It is worth noting that, in practice, the size of PDs is on the order of several millimeters, being much larger than the airy width of the received optical beam. This beam is approximately equal to 2.4λ , where λ is the optical wavelength and lies in the range of a few hundred nanometers. Hence, it is reasonable to ignore the effect of boundary conditions on the four-quadrant detector [4], [13]. As a result, if the deviated received beam is still within the receiver FoV, it will be captured by the i th quadrant of the PD. Moreover, $n_i[k]$ in (1) denotes the noise of the i th quadrant and it is an additive white Gaussian noise (AWGN) having mean zero and variance

$$\sigma_{i,k}^2 = \sigma_s^2 h D_i s[k] + \sigma_0^2, \quad \text{for } i \in \{1, \dots, 4\} \quad (2)$$

where σ_s^2 denotes the variance of the shot noise due to transmitted signal; We have $\sigma_0^2 = \sigma_b^2 + \sigma_{th}^2$ where σ_b^2 and σ_{th}^2 denote the noise variance due to undesired background radiation and receiver thermal noise, respectively. Let us define Ω_{FoV} as the solid angle FoV of the receiver; therefore, the collected background power, P_b , is obtained as [14]

$$P_b = N_b(\lambda) B_o \Omega_{FoV} A_a \quad (3)$$

where $N_b(\lambda)$ (in Watts/cm²-μm-srad) denotes the spectral radiance of the background radiations at wavelength λ , B_o (in μm) denotes the bandwidth of the optical filter at the Rx, and A_a (in cm²) denotes the lens area. To calculate Ω_{FoV} , we denote $\theta_{FoV} = \frac{2r_a}{f_c}$ by the range of optical beam arrival angles observed by the PD area. Here, r_a denotes the radius of the quadrants, and f_c denotes the focal length of the receiver lens. Accordingly, Ω_{FoV} can be obtained as

$$\Omega_{FoV} = \int_0^{\frac{\pi}{2}} \int_0^{\frac{\theta_{FoV}}{2}} \sin(\theta) d\theta d\phi = \frac{\pi}{2} \left(1 - \cos\left(\frac{\theta_{FoV}}{2}\right) \right) \simeq \frac{\pi r_a^2}{4f_c^2}. \quad (4)$$

Hence, in the considered setup, P_b is obtained as

$$P_b = \frac{\pi r_a^2 N_b(\lambda) B_o A_a}{4f_c^2}. \quad (5)$$

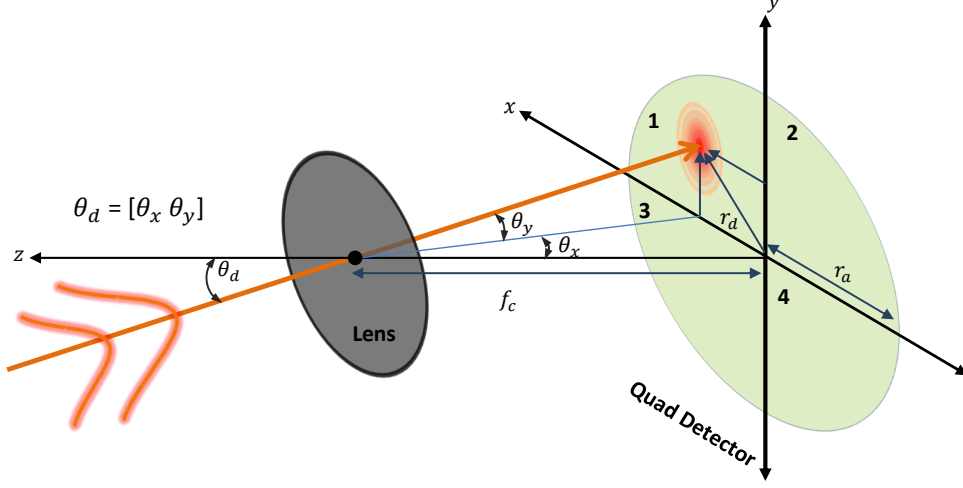


Fig. 1: The schematic of deviated received beam due to the UAV's wobbling at the plane of the four-quadrant detector is depicted. Here, f_c is the focal length of the receiver lens, r_a is the radius of the quadrants, and r_d is the radial beam displacement at the detector array. Furthermore, θ_x and θ_y represent the orientation deviations of received optical beam at $x - z$ and $y - z$ planes, respectively.

B. FSO Channel Model

The channel coefficient can be modeled as $h = h_l h_a h_p$, where h_l is the deterministic attenuation loss, h_a denotes the atmospheric turbulence, and h_p is the pointing error. The probability density function (PDF) of h is given by [15]

$$f_h(h) = \frac{\alpha\beta\gamma^2}{A_0 h_l \Gamma(\alpha)\Gamma(\beta)} \times G_{1,3}^{3,0} \left(\frac{\alpha\beta}{A_0 h_l} h \left| \begin{matrix} \gamma^2 \\ \gamma^2 - 1, \alpha - 1, \beta - 1 \end{matrix} \right. \right) \quad (6)$$

where $G_{1,3}^{3,0}(\cdot)$ and $\Gamma(\cdot)$ denote the Meijer's G function and the Gamma function, respectively. The parameter γ denotes the ratio between the equivalent beam radius at the receiver and the pointing errors jitter, and the parameter A_0 is the maximal fraction of the collected power. Furthermore, $1/\beta$ and $1/\alpha$ are, respectively, the variances of the small scale and large scale eddies, and they can be determined using the Rytov variance [15].

C. Beam Deviation Due to The Hovering Fluctuations

As depicted in Fig. 1, we define two independent random variables (RVs), namely θ_x and θ_y , to model the orientation deviations of received optical beam at the receiver plane.

According to [14], these two RVs are Gaussian distributed with mean zero and variances σ_x^2 and σ_y^2 , when their joint PDF is obtained as

$$p_{\theta}(\theta_x, \theta_y) = \frac{1}{2\pi\sigma_x\sigma_y} \exp\left(-\frac{\theta_x^2}{\sigma_x^2} - \frac{\theta_y^2}{\sigma_y^2}\right). \quad (7)$$

The full beam misalignment will occur if the orientation of the received optical beam, $\theta_d = \sqrt{\theta_x^2 + \theta_y^2}$, deviates bigger than the receiver FoV. Such condition implies $D_i = 0$ for $i \in \{1, \dots, 4\}$. The occurrence probability of full beam misalignment is defined as

$$P_f = 1 - \sum_{i=1}^4 P_{D_i} \quad (8)$$

where P_{D_i} is the probability of capturing the arrival beam at the i th quadrant. Due to the symmetric shape of the detector we have $P_{D_i} = P_{D_j}$ for i and $j \in \{1, \dots, 4\}$, and, for example, P_{D_1} can be attained as

$$\begin{aligned} P_{D_1} &= \int_0^{\tan^{-1}\left(\frac{r_a}{f_c}\right)} \int_0^{\tan^{-1}\left(\frac{r_a}{f_c}\right)} p_{\theta}(\theta_x, \theta_y) d\theta_x d\theta_y \\ &= \left(\frac{1}{2} - Q\left(\frac{\tan^{-1}\left(\frac{r_a}{f_c}\right)}{\sigma_x}\right)\right) \left(\frac{1}{2} - Q\left(\frac{\tan^{-1}\left(\frac{r_a}{f_c}\right)}{\sigma_y}\right)\right). \end{aligned} \quad (9)$$

III. BEAM TRACKING

The received data is gathered during an observation window comprised of L_s bits, i.e., $\mathbf{r}_i = \{r_i[1], r_i[2], \dots, r_i[L_s]\}$ at the i th quadrant of the quad-detector and corresponding to the transmitted signal vector $\mathbf{s} = \{s[1], s[2], \dots, s[L_s]\}$. Due to the slow fading characteristic of the FSO channel, the channel fading h can be estimated at the receiver using either pilot symbols or blind methods.

Let $m = \sum_{k=1}^{L_s} s[k]$ be the number of bits ‘1’ in the vector of transmitted signal. Therefore, at the i th quadrant, the received signal conditioned on h and m can be written as

$$r'_{i|h,m} = \sum_{k=1}^{L_s} r_i[k] = hD_i m + n'_{i|h,m,D_i} \quad (10)$$

where $n'_{i|h,m,D_i} = \sum_{k=1}^{L_s} n_i[k]$ denotes the AWGN with mean zero and variance as

$$\sigma_{i|h,m,D_i}^2 = \sigma_s^2 h D_i m + L_s \sigma_0^2. \quad (11)$$

Thus, the PDF of $r'_{i|h,m}$ conditioned on D_i can be written as

$$p(r'_{i|h,m}|D_i) = \frac{1}{\sqrt{2\pi\sigma_{i|h,m,D_i}^2}} \exp\left(-\frac{(r'_{i|h,m} - hD_i m)^2}{2\sigma_{i|h,m,D_i}^2}\right). \quad (12)$$

For optimum beam tracking, the decision on selecting the i th quadrant as the target quadrant capturing the received optical beam is made based on the maximum likelihood (ML) criterion as follows

$$\begin{aligned}\hat{i} &= \arg \max_{i \in \{1, \dots, 4\}} p(r'_{i|h,m} | D_i = 1) \times \prod_{j=1, j \neq i}^4 p(r'_{j|h,m} | D_j = 0) \\ &= \arg \max_{i \in \{1, \dots, 4\}} \log \left(p(r'_{i|h,m} | D_i = 1) \right) + \sum_{j=1, j \neq i}^4 \log \left(p(r'_{j|h,m} | D_j = 0) \right).\end{aligned}\quad (13)$$

Substituting (12) into (13), after some mathematical derivations, we can express the optical beam tracking based on the metric $\mathcal{T}_{i|h,m}$ as

$$\hat{i} = \arg \min_{i \in \{1, \dots, 4\}} \mathcal{T}_{i|h,m} \quad (14)$$

where

$$\mathcal{T}_{i|h,m} = \frac{|r'_{i|h,m} - hm|^2}{\sigma_s^2 hm + L_s \sigma_0^2} + \sum_{j=1, j \neq i}^4 \frac{|r'_{j|h,m}|^2}{L_s \sigma_0^2}. \quad (15)$$

The probability of tracking error for the proposed method is derived in Appendix A as

$$\begin{aligned}P_{te}^p &\simeq P_f + \frac{(1 - P_f)}{2^{L_s}} \int_0^\infty \sum_{m=0}^{L_s} \binom{L_s}{m} \\ &\left\{ 1 - \left(1 - Q \left(\frac{\sigma_s^2 h^2 m^2 (hm + 2L_s \sigma_0^2)}{\sigma_{tc|h,m}} \right) \right)^3 \right\} f_h(h) dh\end{aligned}\quad (16)$$

where

$$\begin{aligned}\sigma_{tc|h,m}^2 &= (2\sigma_s^2 hm (hm + L_s \sigma_0^2))^2 \cdot (\sigma_s^2 hm + L_s \sigma_0^2) \\ &+ L_s \sigma_0^2 (2m L_s \sigma_0^2 \sigma_s^2 h)^2.\end{aligned}\quad (17)$$

IV. SIMULATION RESULTS AND DISCUSSION

We provide simulation results to investigate the effect of hovering fluctuations and the detector size on the performance of considered system. Moreover, the accuracy of analytical analysis is corroborated by performing 6×10^6 independent runs through Monte-Carlo simulations. For simulations, we set the parameter values as follows [14]. Rytov variance = 1, aperture radius = 5 cm, $f_c = 5$ cm, $N_b(\lambda) = 10^{-3}$ W/cm²-m-srad, $B_o = 10$ nm, and $A_0 = 0.0198$. Fig. 2 depicts tracking error versus P_t for different values of L_s . As we can observe, increasing L_s improves the performance of the tracking method at the expense of more delay of tracking. However, an error floor for tracking error is realized due to the transmission of all-zero sequence having the occurrence probability $1/2^{L_s}$. Nevertheless, this error can be avoided by adopting a source preceding method at the transmitter [16]. Furthermore, the dramatic impact of hovering fluctuations on the proposed tracking approach

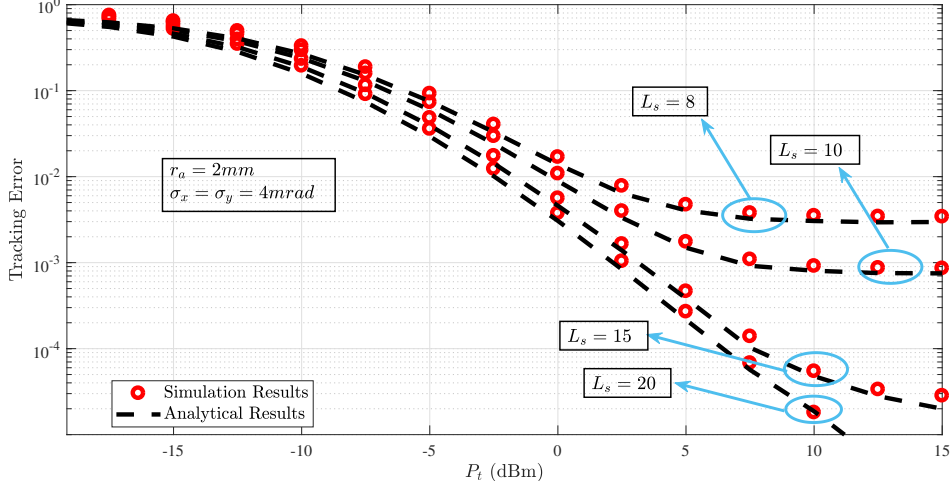


Fig. 2: Tracking error versus P_t for different values of L_s

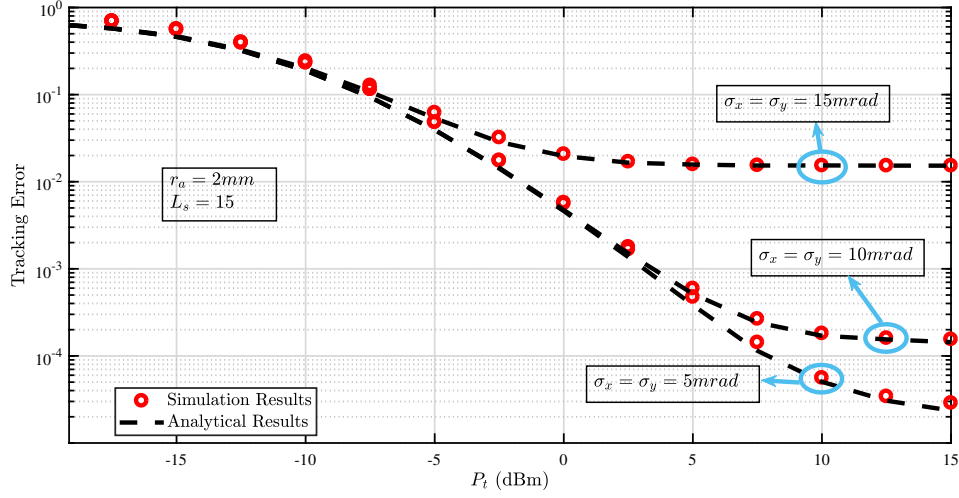


Fig. 3: Tracking error versus P_t for different values of σ_x and σ_y

is reflected in Fig. 3. However, this negative impact can be compensated by enlarging the size of the PD at the receiver, which increases the Rx FoV.

Moreover, Fig. 4 plots tracking error versus detector size for different values of hovering fluctuations. As shown, widening the receiver FoV by using larger PDs can help compensate tracking error at the expense of less electrical bandwidth and accept more undesired background noise at the receiver. Meanwhile, Fig. 4 demonstrates that for each level of instability there exist an optimal size of the detector that can minimize the tracking error probability. Furthermore, to demonstrate the impact of detector size on the overall system performance, we plot the BER versus transmit power for different radius of the quadrants in Fig. 5. Again,

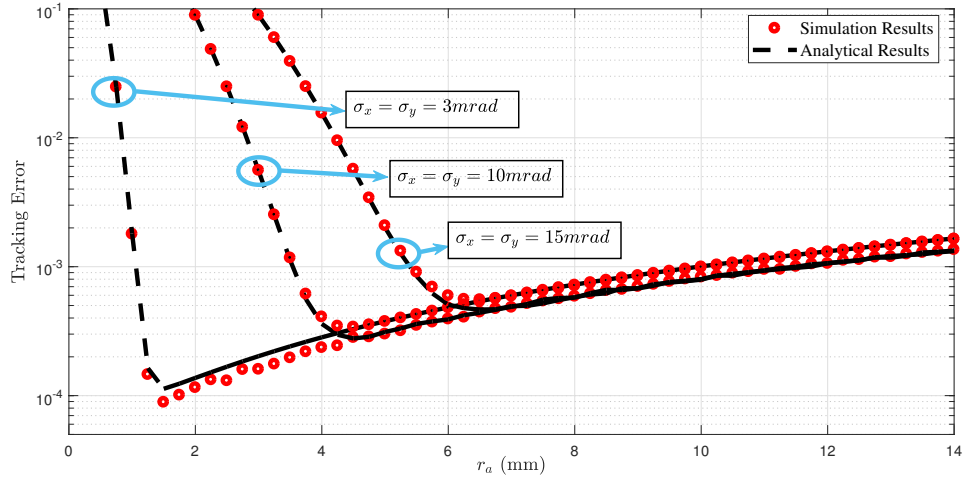


Fig. 4: Tracking error versus detector size for different values of σ_x and σ_y

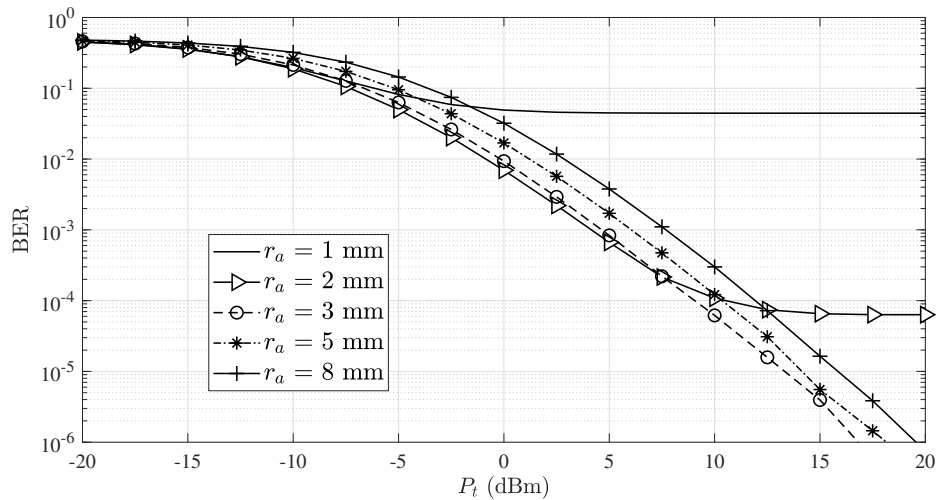


Fig. 5: BER versus P_t for different values of detector size r_a , when $\sigma_x = \sigma_y = 5$ mrad, $L_s = 20$

it can be seen from this figure that increasing the size of the quadrants can help mitigate the adverse effect of AoA fluctuations on the system performance. However, from a certain size onward ($r_a = 5$ mm in this figure), further increase does not necessarily improve the system performance. This observation is expected, because increasing the detector size results in accepting more undesired background noise due to a wider receiver FoV. Furthermore, for the small sizes of the detector and from a certain level of transmit power onward, increasing the power does not necessarily have a noticeable effect on improving the system performance. In this case, the system performance is limited to the tracking error, and when the detector

size is small, the amount of this error cannot be reduced to an acceptable level, resulting in an error floor.

V. CONCLUSION

We investigated the effect of random hovering fluctuations on the performance of beam tracking method for an FSO link to a UAV. Extensive mathematical analysis was carried out, and a semi-closed form expression for the tracking error probability was derived. Our analytical method can find the optimal detector size for minimizing tracking error without resorting to time-consuming simulations.

APPENDIX A

TRACKING ERROR ANALYSIS

For the proposed method, tracking error is expressed as

$$P_{te} = P_f + (1 - P_f) \int_0^\infty P_{te|h} f_h(h) dh \quad (18)$$

where

$$P_{te|h} = \sum_{m=0}^{L_s} p(m) P_{te|h,m}^p \quad (19)$$

$$P_{te|h,m}^p = 1 - P_{tc|h,m}^p. \quad (20)$$

We have $P_{te|h,m}^p$ and $P_{tc|h,m}^p$ as the tracking error probability and the probability of correct tracking conditioned on h and m , respectively. Furthermore, $P(m) = \binom{L_s}{m}/2^{L_s}$ denotes the probability that m bits out of L_s transmitted bits are equal to one where $\binom{n}{m}$ is the number of combinations of m items out of n items. Without loss of generality, we assume that the first quadrant is the target PD, i.e., $D_1 = 1$. Then, we have

$$P_{tc|h,m}^p = \text{Prob} \{ \mathcal{T}_1|_{h,m} < \mathcal{T}_{\min|_{h,m}} \} \quad (21)$$

where

$$\mathcal{T}_{\min|_{h,m}} = \min (\mathcal{T}_2|_{h,m}, \mathcal{T}_3|_{h,m}, \mathcal{T}_4|_{h,m}). \quad (22)$$

The noise of the PDs are independent; therefore (21) simplifies to

$$P_{tc|h,m}^p = \left(P_{tc|h,m}^{i,p} \right)^3 \quad (23)$$

where

$$P_{tc|h,m}^{i,p} = \text{Prob} \{ \mathcal{T}_1|_{h,m} < \mathcal{T}_i|_{h,m} \} \text{ for } i \in 2, 3, 4. \quad (24)$$

Substituting (15) into (24), we can express $P'_{tc|h,m}$ as (25) at the bottom of this page. From (10), eq. (25) is rewritten as

$$\begin{aligned} P'_{tc|h,m} &= \text{Prob} \left\{ \sigma_s^2 h m \left(\left(h m + n'_{1|h,m,D_1=1} \right)^2 - \left(n'_{2|h,m,D_2=0} \right)^2 \right) \right. \\ &\quad \left. + 2 m L_s \sigma_0^2 \sigma_s^2 h \left(h m + n'_{1|h,m,D_1=1} - n'_{2|h,m,D_2=0} \right) > 0 \right\} \\ &= \text{Prob} \left\{ \sigma_s^2 h^2 m^2 (h m + 2 L_s \sigma_0^2) + n'_{tc|h,m} > 0 \right\} \end{aligned} \quad (26)$$

where

$$\begin{aligned} n'_{tc|h,m} &= \sigma_s^2 h m \left(\left(n'_{1|h,m,D_1=1} \right)^2 - \left(n'_{2|h,m,D_2=0} \right)^2 \right) \\ &\quad + 2 \sigma_s^2 h m \left(h m + L_s \sigma_0^2 \right) n'_{1|h,m,D_1=1} \\ &\quad - 2 m L_s \sigma_0^2 \sigma_s^2 h n'_{2|h,m,D_2=0}. \end{aligned} \quad (27)$$

At high SNR, we have $\left(n'_{1|h,m,D_1=1} \right)^2 \ll n'_{1|h,m,D_1=1}$ and $\left(n'_{2|h,m,D_2=0} \right)^2 \ll n'_{2|h,m,D_2=0}$. Hence, eq. (27) can be approximated as

$$\begin{aligned} n'_{tc|h,m} &\simeq 2 \sigma_s^2 h m \left(h m + L_s \sigma_0^2 \right) n'_{1|h,m,D_1=1} \\ &\quad - 2 m L_s \sigma_0^2 \sigma_s^2 h n'_{2|h,m,D_2=0}. \end{aligned} \quad (28)$$

From (28) and (11), $n'_{tc|h,m}$ can be described by a Gaussian distribution with mean zero and variance

$$\begin{aligned} \sigma_{tc|h,m}^2 &= \left(2 \sigma_s^2 h m \left(h m + L_s \sigma_0^2 \right) \right)^2 \times \left(\sigma_s^2 h m + L_s \sigma_0^2 \right) \\ &\quad + L_s \sigma_0^2 \left(2 m L_s \sigma_0^2 \sigma_s^2 h \right)^2. \end{aligned} \quad (29)$$

Based on (29) and (26), $P'_{tc|h,m}$ is derived as

$$P'_{tc|h,m} \simeq 1 - Q \left(\frac{\sigma_s^2 h^2 m^2 (h m + 2 L_s \sigma_0^2)}{\sigma_{tc|h,m}} \right). \quad (30)$$

Finally, by substituting (30), (23), (20), and (19) into (18), we obtain the analytical expression of tracking error probability in (16).

$$\begin{aligned} P'_{tc|h,m} &= \text{Prob} \left\{ \frac{|r'_{1|h,m} - h m|^2}{\sigma_s^2 h m + L_s \sigma_0^2} + \sum_{j=2}^4 \frac{|r'_{j|h,m}|^2}{L_s \sigma_0^2} < \frac{|r'_{2|h,m} - h m|^2}{\sigma_s^2 h m + L_s \sigma_0^2} + \frac{|r'_{1|h,m}|^2}{L_s \sigma_0^2} + \sum_{j=3,4} \frac{|r'_{j|h,m}|^2}{L_s \sigma_0^2} \right\} \\ &= \text{Prob} \left\{ \sigma_s^2 h m \left((r'_{1|h,m})^2 - (r'_{2|h,m})^2 \right) + 2 m L_s \sigma_0^2 \sigma_s^2 h (r'_{1|h,m} - r'_{2|h,m}) > 0 \right\} \end{aligned} \quad (25)$$

REFERENCES

- [1] H. Wang *et al.*, “Deployment algorithms of flying base stations: 5G and Beyond With UAVs,” *IEEE Internet Things J.*, vol. 6, no. 6, pp. 10 009–10 027, Dec. 2019.
- [2] M. Alzenad, M. Z. Shakir, H. Yanikomeroglu, and M.-S. Alouini, “FSO-based vertical backhaul/fronthaul framework for 5G+ wireless networks,” *IEEE Commun. Mag.*, vol. 56, no. 1, pp. 218–224, Jan. 2018.
- [3] H. Safi, A. Dargahi, J. Cheng, and M. Safari, “Analytical channel model and link design optimization for ground-to-hap free-space optical communications,” *IEEE/OSA J. Lightw. Technol.*, vol. 38, no. 18, pp. 5036–5047, Sep. 2020.
- [4] R. Gagliardi and S. Karp, *Optical Communications*. New York: Wiley, 1995.
- [5] Y. Kaymak, R. Rojas-Cessa, J. Feng, N. Ansari, M. Zhou, and T. Zhang, “A survey on acquisition, tracking, and pointing mechanisms for mobile free-space optical communications,” *IEEE Commun. Surveys Tuts.*, vol. 20, no. 2, pp. 1104–1123, Feb. 2018.
- [6] W. Zhang, W. Guo, C. Zhang, and S. Zhao, “An improved method for spot position detection of a laser tracking and positioning system based on a four-quadrant detector,” *Sensors*, vol. 19, no. 21, p. 4722, Jan. 2019.
- [7] M. S. Bashir and M. R. Bell, “Optical beam position tracking in free-space optical communication systems,” *IEEE Trans. Aerosp. Electron. Syst.*, vol. 54, no. 2, pp. 520–536, July 2017.
- [8] M. S. Bashir, “Free-space optical communications with detector arrays: A mathematical analysis,” *IEEE Trans. Aerosp. Electron. Syst.*, vol. 56, no. 2, pp. 1420–1429, Sep. 2019.
- [9] M. S. Bashir, M.-C. Tsai, and M.-S. Alouini, “Cramér–Rao bounds for beam tracking with photon counting detector arrays in free-space optical communications,” *IEEE Open J. Commun. Soc.*, vol. 2, pp. 1065–1081, May 2021.
- [10] M. S. Bashir and M.-S. Alouini, “Beam tracking with photon-counting detector arrays in free-space optical communications,” *arXiv preprint arXiv:2001.04007*, 2020.
- [11] Z. Ghassemlooy, W. Poopola, and S. Rajbhandari, *Optical Wireless Communications: System And Channel Modelling With Matlab*. CRC Press, 2019.
- [12] H. R. Burris *et al.*, “Large diameter high-speed InGaAs receivers for free-space lasercom,” in *Atmospheric Propagation IV*, vol. 6551. International Society for Optics and Photonics, 2007, p. 65510P.
- [13] K. Kiasaleh, “Beam-tracking in FSO links impaired by correlated fading,” in *Free-Space Laser Communications VI*. International Society for Optics and Photonics, Sep. 2006.
- [14] M. T. Dabiri, S. M. S. Sadough, and M. A. Khalighi, “Channel modeling and parameter optimization for hovering UAV-based free-space optical links,” *IEEE J. Sel. Areas Commun.*, vol. 36, no. 9, pp. 2104–2113, Sep. 2018.
- [15] H. G. Sandalidis, T. A. Tsiftsis, and G. K. Karagiannidis, “Optical wireless communications with heterodyne detection over turbulence channels with pointing errors,” *IEEE/OSA J. Lightw. Technol.*, vol. 27, no. 20, pp. 4440–4445, Oct. 2009.
- [16] L. Yang, B. Zhu, J. Cheng, and J. F. Holzman, “Free-space optical communications using on–off keying and source information transformation,” *IEEE/OSA J. Lightw. Technol.*, vol. 34, no. 11, pp. 2601–2609, June 2016.